Nitrogen Flow Effects on Part Bed Surface Temperature during Laser Sintering

Mengqi Yuan* and David Bourell*

*Laboratory for Freeform Fabrication, Mechanical Engineering Department
The University of Texas at Austin, TX 78712
Accepted August 16th 2013

Abstract

The role of nitrogen flow rate was invested as it affects the surface temperature of a polymer laser sintering part bin. A SinterStation 2500® was used for this study. The effect of nitrogen chamber flow rates between 0.5 and 2.5 m^3/hr was observed and compared to the results of a computational fluids dynamics model. Increasing convective flow generates a uniform reduction in the surface temperature, but it does not meaningfully reduce surface temperature gradients. The part bin piston was modified to allow down drafting of nitrogen through the part bin. Down drafting, while once considered to be effective in accelerating cooling at the end of builds, did not have a significant effect on the surface temperature profile.

Introduction

Laser sintering (LS) is an additive manufacturing technology that uses a laser to fuse polymer powder into a mass that has a desired three-dimensional shape. After one surface layer is laser scanned, a new layer of fresh powder is added on the powder bed, creating a new layer that is scanned. The process is repeated until the part is completed [1]. Polyamide 12, also known as Nylon 12, is a thermoplastic material that is widely used in laser sintering. It has high elongation, good abrasion resistance, good specific strength and melts at a temperature around 180°C [1].

No systematic study of nitrogen effect on the laser sintered part bed has been conducted before. Instead, temperature distribution of powder bed during LS has been analyzed in different materials including metal, polymer, etc. Some were focused on the surface temperature distribution, while others focused on the LS operation chamber. S. Kolossov *et.al* [2] developed a 3D thermal model of LS using finite element simulation, which incorporated the nonlinear behavior of the titanium powder. They found the temperature profiles during LS operation along both X- and Y- axes reached a maximum around 2500°C in the middle of the axes, and decreased to 500- 750°C on both sides. These results were in agreement with the infrared red camera experiments. Moreover, the only temperature profile examined was during the stable heat-up period; it is unknown how the part bed temperature profile behaved during LS processing which is an important part of the overall thermal exposure.

Downdraft is an approach to reduce the hottest spot surface temperature and to create a uniform sintered part cake temperature. It manages cooling rate in the entire part cake by percolating cold nitrogen through the porous cake [3]. Paul *et.al* [3] developed downdraft on the SinterStation using a design of experiments (DOE) approach, with experimental designs running

with the input variables being piston temperature and downdraft flowrate, and the output of the experimental design was part wrap since the cooling rate is difficult to measure [3]. It showed a decrease in part wrap as downdraft flowrate increased; it also showed that percolation of heated gas was one of the few practical methods to redistribute heat in the part cake.

In this research effort, A SinterStation 2500® was used. The thermal profile of the SinterStation was investigated, and the part bed heater was modified. The role of nitrogen flow rate was invested as it affects the surface temperature of a polymer laser sintering part bin. The effect of nitrogen chamber flow rates between 0.5 and 2.5 m^3/hr was observed and compared to a computational fluids dynamics model. The part bin piston was modified to allow down drafting of nitrogen through the part bin. Downdraft effects were analyzed.

Experimental Procedure

2.1 Thermal profile investigation

Temperature measurements at the surface of the part bed were made using a FLIR infrared (IR) camera. For the measurement, the camera temperature range was 0-500 °C, yielding a thermal resolution of 0.03 °C. Absolute accuracy of the camera was 2 °C for known emissivity. The insulated viewing window in front of the SS2500® was replaced with an insulated aluminum-fiberglass panel with visible and IR transparent zinc-selenide (ZnSe) viewports. The IR camera was mounted at the front of the machine and sighted through the viewports. The ZnSe window had an anti-reflective coating for a transmissivity greater than 0.98 [4]. The camera was enclosed in a fan-cooled box to protect it from dust and powder. The camera was controlled by FLIR ExaminIR software. Figure 1 shows a representative thermograph from the IR camera of a heated chamber, with the nonlinear temperature scale in °C.

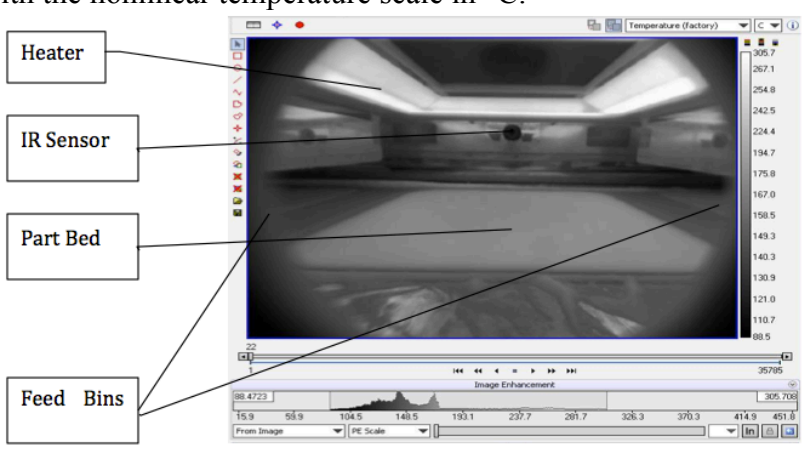

Figure 1: LS chamber in the SinterStation 2500® captured by the IR camera. Visible are the radiant heater, IR sensor, part bed and two feed bins.

2.2 Heater temperature uniformity

The non-uniform heating of the part bed heater has an effect on the part bed surface temperature. A WATLOW ceramic fiber patch kit was used to cure the right-down hot corner of the part bed heater. Black surface powder and rigidizer were mixed at a one-to-one ratio and

applied onto the patched area. Thermographs were taken of the radiant heater before and after the fix, after heating for 15 minutes. Thermographs were also made of the part bed surface during heating with temperature increasing to 170 °C.

2.3 Nitrogen circulation effect

To analyze the circulating nitrogen thermal effect on the part bed surface temperature, the part bed was heated to 175 °C. First the nitrogen flow rate was changed from 0.5 m^3/h to 2.5 m^3/h, increased by 0.5 m^3/h incrementally and held for 5 minutes. A line in the middle of the part bed along the X- axis was observed by the IR camera to obtain a thermal profile. After this, the circulating nitrogen valve was closed, and the IR camera observed the line for 1 hour. Thermal profiles were plotted along the X- axis at different time periods.

2.4 Downdraft

Downdraft was another approach to create a uniform sintered part cake temperature. It manages cooling rate in the entire part cake by percolating cold nitrogen through the porous cake [3]. As shown on the Fig. 2 below, a woven wire cloth (30.5 cm by 71cm, mesh size 400, 0.0254 mm wire diameter) was used to cover the part bed piston surface. It prevented the powder from falling down past the piston. An aluminum tube was mounted under the piston and connected to a pump. The pump nitrogen intake rate was 10 L/min. Two thermocouples were installed on the piston to record the part cake temperature during the build, one near the intake tube that is in the middle of the surface, and one at the corner. The IR camera was mounted to acquire the temperature change on the hottest spot, coldest spot, and part bed mean temperature. To evaluate the downdraft effect, two tensile bars were built, one each on the hot spot and cold spot with downdraft working. The nitrogen flow rate was 7 L/min; after 0.2 inch layer powder separation, two more bars were built on the same position but without the downdraft. The second experiment then conducted in a reverse way: no downdraft first then downdraft working.

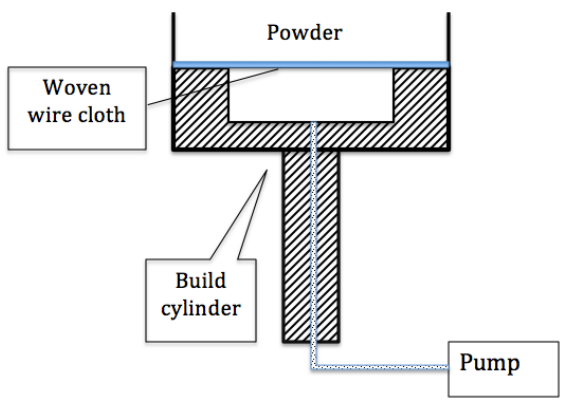

Figure 2: Sketch of the cross section of the downdraft on the 2500® SinterStation.

Results and Discussion

3.1 Thermal profile investigation

Temperature changes at every stage (warm-up, LS and cool-down) were recorded by the IR camera and processed by MATLAB. An IR image of LS on the powder bed surface is shown in Fig. 3. There was a 10-15 °C temperature difference on the powder bed surface between the hottest spot and coldest spot. The heater is shown all white because its temperature falls outside the measurement range. The part bed surface is hot in the middle and right corner, but cold around four sides and the upper-left corner. Convection from the environment may contribute to the thermal gradient.

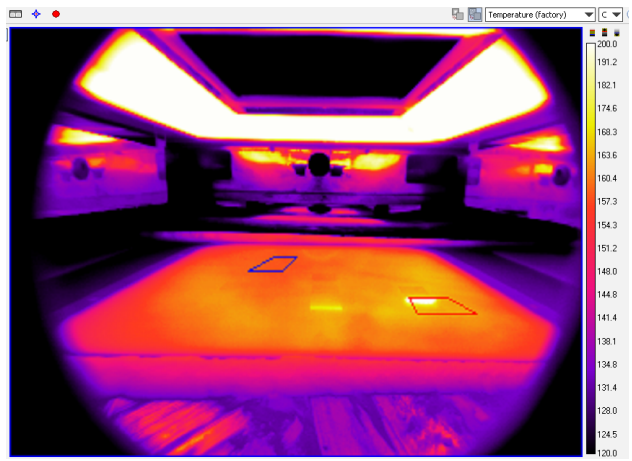

Figure 3: Thermograph from the IR camera during laser sintering. Default emissivity is set as 0.825. The temperature range was manually set to be 120- 200 °C. Two squares drawn on the surface (lower right and upper left) show a hot spot and cold spot of powder bed, respectively. The bright yellow rectangle in the middle of the part bed surface is a square that just finished being laser sintered. The brighter white rectangular spot on right was being laser sintered when the image was captured.

Figure 4a-c show powder bed surface temperature profiles during laser sintering that were recorded, exported by FLIR camera and processed by MATLAB.

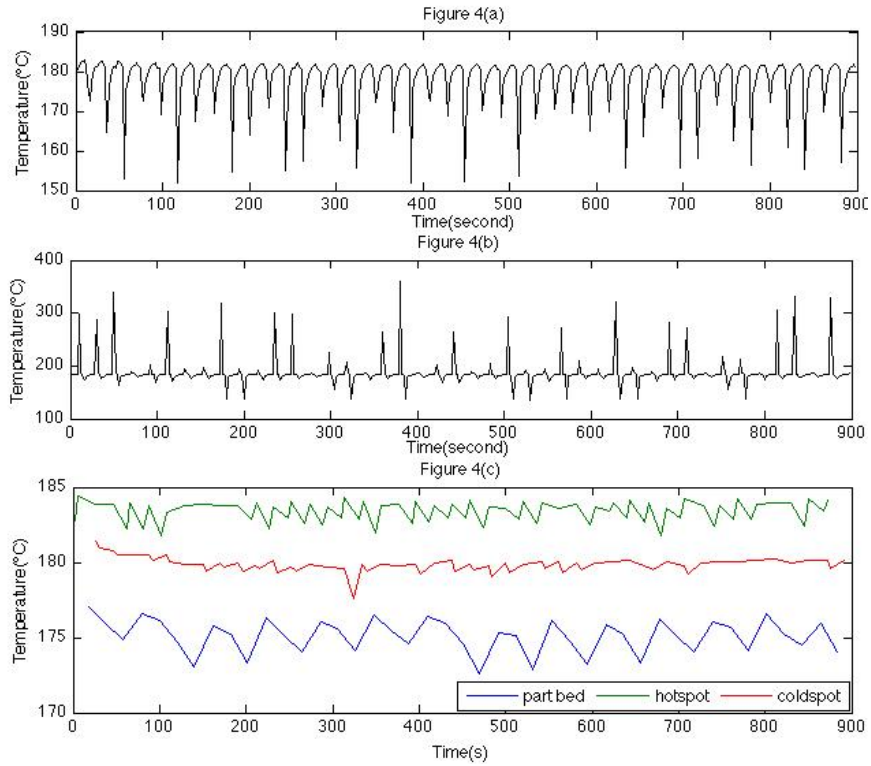

Figure 4: Polyamide 12 part bed surface temperature profile versus time during laser sintering. (a) The mean temperature of part bed surface during LS; (b) The mean temperature profile of hot spot surface during LS; (c) The mean temperature profile processed by MATLAB that includes the mean surface temperature profiles versus time for the part bed, hot spot and cold spot.

Figure 4a shows a thermal recording from the IR camera versus time for the part bed surface mean temperature during LS. A large temperature gap occurred after each 70-80 seconds indicating the moment the roller spread the powder over the surface, while the mean temperature dropped to 152-153 °C.

Figure 4b is the real-time IR record showing the hot spot mean temperature on the part bed surface versus time. The high temperatures shown (300-400 °C) were not reasonable since the part was in a melt or half-melt status, and the emissivity was changed, rendering the measurement to be inaccurate. However, it still seen that the LS process temperature was decreased by the roller spreading powder over the surface and was increased by LS.

Figure 4c shows the mean temperature profile versus time processed by MATLAB of the whole part bed, hot spot, and cold spot during the whole LS process. Each data point was selected at the moment after LS when the temperature reached equilibrium. However, the temperature data for the hot spot and cold spot were higher than 180 °C because the part was still in a “half melt” status with the emissivity changed from 0.825. In addition, the system error was included (2 °C) [6]. It is seen that the hot spot temperature was 3-5 °C higher than that of the cold spot. The part bed mean temperature was lower than both spots at around 175°C, which is quite close to the set point.

3.2 Heater temperature uniformity

To reduce the thermal gradient on the part bed surface, the radiant heater was modified to ensure providing uniform heat on the surface. It was disassembled from the SinterStation, heated 15 minutes vertically on a metal stand, and images were captured by IR camera as shown in Fig. 5. These two images have different thermal scales: 300-592.5 °C for Figure. 5a and 295.2-360 °C for Figure. 5b. Figure 5a shows the temperature difference before curing was around 30 °C, while 5b shows the difference after curing was 7°C. Figure. 6 shows the part bed center line (along x-axis) temperature before and after radiant heater curing. A peak about 183 °C was shown in the area of x = 300~350mm; however, after the heater was cured, it decreased to 180°C. The lowest temperature was shown on the area of x=250 mm on both profiles.

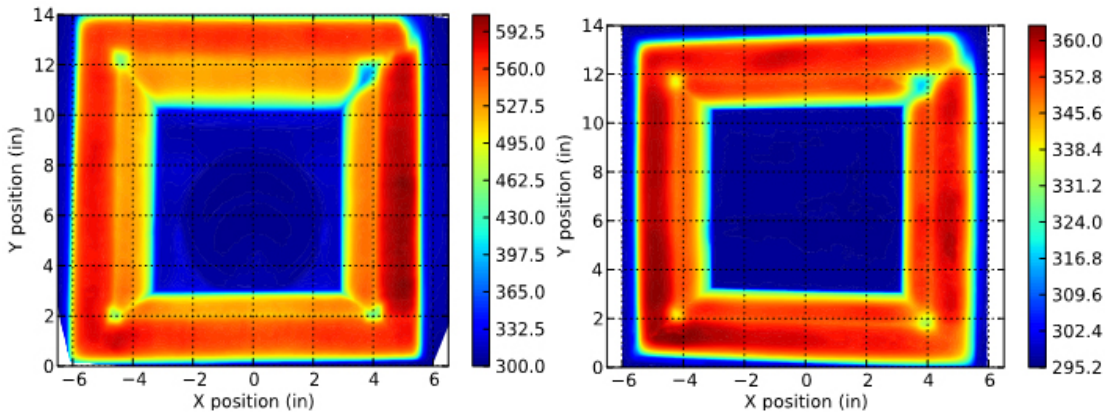

Figure 5: Thermograph from the IR camera for the part bed radiant heater (a) before curing; (b) after curing. Temperatures are in Kelvin.

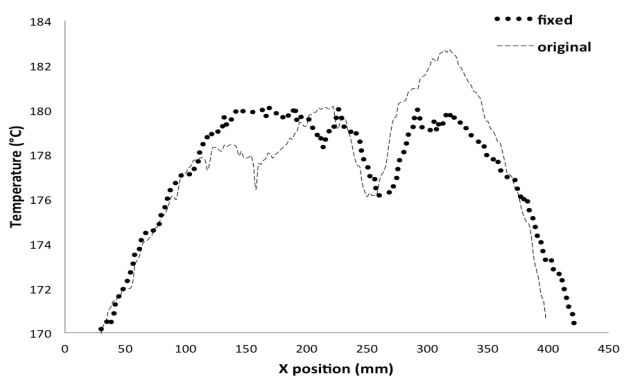

Figure 6: Heater effect on part bed surface temperature. The mean temperature profiles of a part bed surface middle-line along the x-axis, before and after curing the radiant heater.

Figure 5 shows that applying the ceramic fiber patch to hot spots on the radiant heater effectively reduces the heater temperature gradient from 30 °C to 7 °C, and the part bed middle line temperature variation was reduced as well, as shown in Figure 6. However, the cold spot (x =250 mm) cannot be repaired by applying the ceramic patch, and the following thermographs show the ceramic kit effect was eliminated with heating the heater in the LS process, as the

ceramic patch occasionally spalls locally. It is still an effective way to reduce thermal gradients on the part bed surface.

3.3 Nitrogen circulation effect

To analyze nitrogen effects on the part bed profile, two experiments were conducted with the nitrogen purge gas on and purge gas off, respectively, which results are shown below in Figure 7.

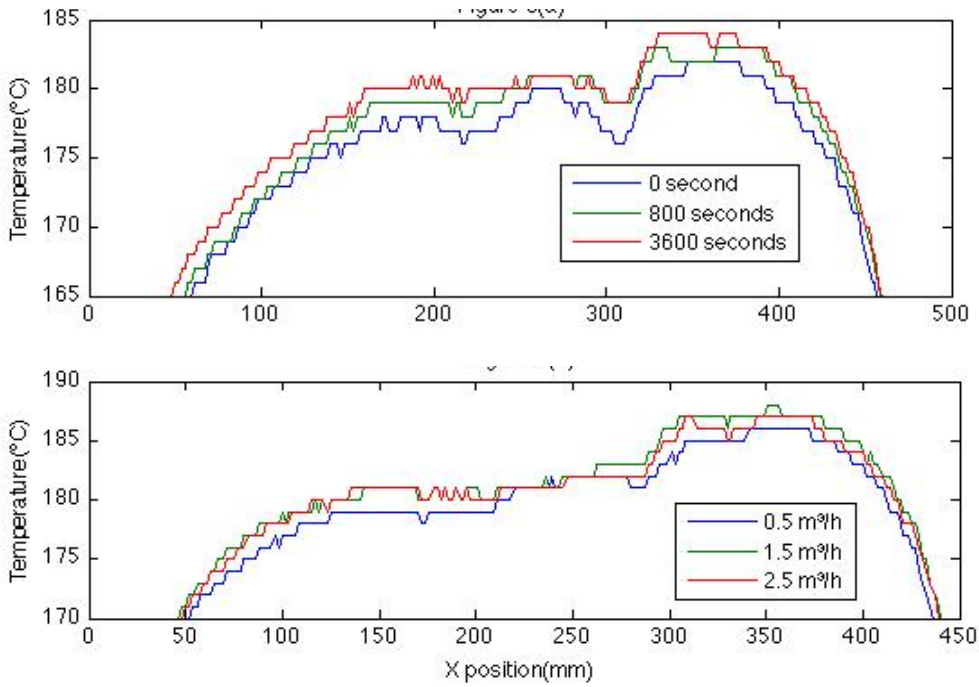

Figure 7: Nitrogen circulation effect on part bed surface temperature. (a) The mean temperature of a part bed surface centre-line along the x-axis with purge nitrogen off at the moment nitrogen was off and 800 and 3600 seconds later; (b) The mean temperature of the part bed surface centre line along the x-axis with purge nitrogen on, at nitrogen rates of 0.5, 1.5, 2.5 m^3/h.

Figure 7a shows that the part bed mean surface temperature increased with time after turning the circulation nitrogen off. The temperature range was selected from 165- 185 °C for better observation. The whole part bed mean temperature increased 2-3 °C after turning nitrogen off for 800 seconds and increased another 2-3 °C after 3600 seconds, in that the nitrogen purged before turning off is heated and contributes heat to the surface part bed.

Figure 7b shows the effect of different nitrogen circulation rates on the whole part bed mean surface temperature. The temperature increased 1-2 °C after changing the nitrogen rate from 0.5 m^3/h to 1.5 m^3/h, and remained when the nitrogen rate was changed from 1.5 m^3/h to 2.5 m^3/h. Data were selected 5 minutes after changing the nitrogen rate. Within the first 5 minutes, nitrogen was continuously purging and heated by the heater. So the heated nitrogen had an effect on the part bed by increasing part bed mean surface temperature. However, the part bed mean surface temperature increased when the nitrogen rate stayed in a small range. After changing the

flow rate to 2.5 m^3/h, the part bed temperature was the same as the part bed temperature when the flow rate was 1.5 m^3/h. Since the nitrogen at this high rate was not completely heated, cold nitrogen caused convection loss on the surface.

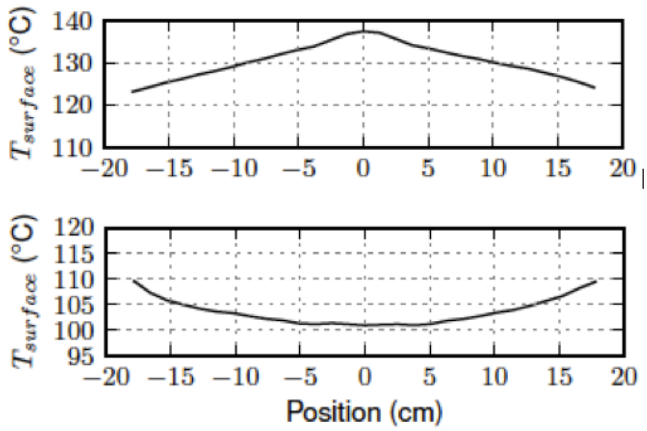

Figure 8: Computed part bed surface temperature profile during warm up after 1600s from a steady state convection 2D model (a) purge gas off; (b) purge gas on with purging rate 0.96 m^3/h. Initial temperature was 60 °C [13].

Figure 7 is compared with Figure 8, which shows the part bed surface temperature profile with and without purging nitrogen from a 2D computational fluid dynamics model [5]. The heated SinterStation was posed as an unsteady finite-difference problem, where the heat flux to the surface could be updated at each step. The finite-element model of the build part bed was created using ANSYS/ GAMBIT. Figure 7a and 8a both show the temperature increases in the middle, while a larger peak was shown on Figure 7a because of the hot spot existing on the right side of the part bed. However the curves of Figure 7b and 8b are inversed. Figure 7b shows the temperature increasing while Figure 8b shows the temperature decreasing from the middle. The conclusion is that the nitrogen circulation method showed promise based on previous computational modeling, but this was not borne out experimentally to be effective in reducing thermal gradients on the part bed.

3.4 Downdraft

Figure 9a shows the mean temperatures on the part bed during LS of the cold spot and hot spot, with and without the nitrogen down drafting. The cold spot temperature became more constant with nitrogen flowing, and the hot spot temperature decreased 2-4°C with downdraft. Figure 9b shows the spot temperatures with reversed experiment procedure (no downdraft first then downdraft working). The cold spot temperature decreased 1-2 °C with nitrogen flowing, while the hot spot temperature remained almost stable at 178-180 °C.

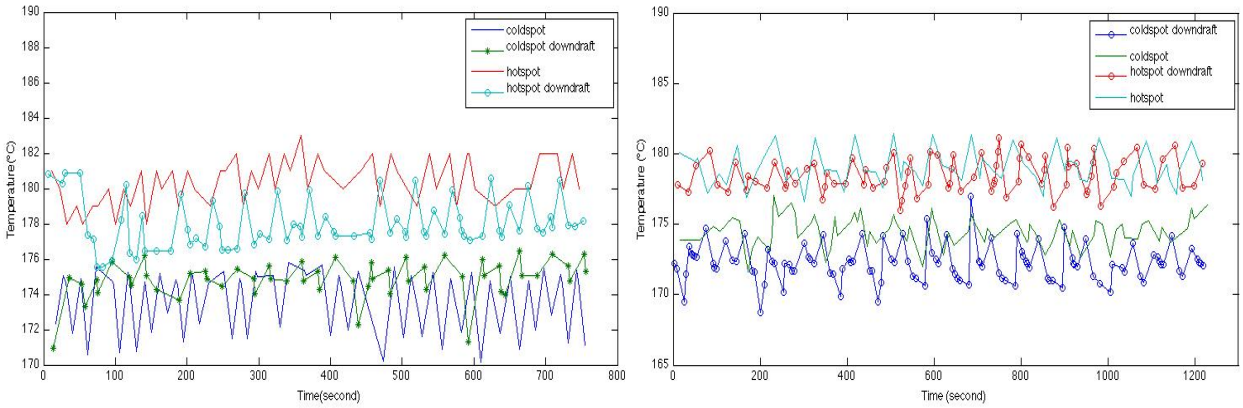

Figure 9: Cold spot and hot spot temperatures on part bed surface during LS with/without nitrogen down drafting (a) downdraft first then no downdraft; (b) no downdraft then downdraft working.

Figure 9 shows that the thermal gradient between the hot spot and cold spot was decreased with cold nitrogen percolation. However the effect was eliminated when conducting the experiment in a reversed way. While down drafting is expected to have potential benefits on post-build factors such as thermal homogenization of the part bed and accelerated cooling of the part bed after the build is complete, the effect on the part bed surface temperature gradients was small.

Summary and Conclusion

In terms of thermal management, various experiments were conducted to investigate and reduce thermal gradients on the part bed during LS. First, the thermal profile investigation provides the actual and MATLAB processed temperature profiles of the part bed surface during the LS stages. Hot spot temperature was 3-5 °C higher than that of the cold spot in LS. Second, minimizing thermal gradients on the radiant heater benefits part bed surface gradient reduction, but the effect did not last since the ceramic patch wore off quickly. Third, the part bed mean surface temperature increases with time after turning the circulation nitrogen off; it increased 1-2 °C after changing the nitrogen rate from 0.5 m^3/h to 1.5 m^3/h, and remained so when the nitrogen rate was changed from 1.5 m^3/h to 2.5 m^3/h. Fourth, nitrogen down drafting on part bed proved ineffective in reducing the part bed surface thermal gradient.

Acknowledgments

The authors would like to acknowledge funding from the Air Force Research Laboratory under Grant #GRT00015778.

References

[1] M. Yuan, T. Diller, D. Bourell (2011), 'Thermal Conductivity Measurements of Polyamide 12', *Solid Freeform Fabrication Symposium Proceeding,* 427-437, Austin, TX.

[2] S. Kolossov, E. Boillat, R. Glardon, P. Fischer, M. Locher, 2003, '3D FE simulation for temperature evolution in the selective laser sintering process', *International Journal of Machine Tools & Manufacture*, Vol. 44, pp. 117-123.

[3]Forderhase. P., MaClea. K., Michalesicz. M., Ganniger M., Firestone K., (1994), 'SLS™ prototypes from nylon', *Solid Freeform Fabrication Symposium*, pp.102-109.

[4] Optics, I, 2010, *BBAR- ZNSE-8-12 Data Sheet*, http:// www.Isoptics.com.

[5] T. Diller, M. Yuan, D. Bourell, J. Beaman, (2011), 'Thermal model and measurements of polymer laser sintering', *Rapid Prototyping Journal*, accepted on April-2013.